Chapter 36
Earthquake Induced Landslides in Lake Éternité, Québec, Canada

Jacques Locat, Dominique Turmel, Marion Habersetzer, Annie-Pier Trottier, Patrick Lajeunesse, and Guillaume St-Onge

Abstract Lake Éternité, located between the Upper Saguenay Fjord and the St. Lawrence River has registered many submarine slides caused by at least one earthquake. Landslides are mostly rooted in the gyttja (Holocene sediments). Mapping of landslides revealed a total of 128 scars over an area of only 3.2 km^2. A larger proportion of the landslide scars are located on the SE and NW facing slope which may support an epicentre location for the strongest earthquake (1663?), to the NW or NE of the lake. The preliminary numerical analysis of the site effects caused by topography on local preferred seismic amplification is not conclusive enough to support the observations made for landslides. Associating landslides to specific earthquakes will only be possible with further investigations, including coring of various features including rupture surfaces. The study also revealed interesting slide morphologies developed in homogeneous sediments, providing excellent examples for future modelling of similar events.

36.1 Introduction

Recent studies have attempted to investigate the morphology and sedimentology of lakes and fjords in Québec and Ontario in order to better define the postglacial seismic records (e.g., Shilts 1984; Doig 1990; Shilts and Clague 1992; Levesque et al. 2006; Lajeunesse et al. 2008; Normandeau et al. 2013; Doughty et al. 2014). Central to this research is the February 5th 1663 earthquake (Lamontagne 1987),

J. Locat (✉) • D. Turmel • M. Habersetzer
Laboratoire d'études sur les risques naturels, Département de géologie et de génie géologique, Université Laval, Québec, QC G1V 0A6, Canada
e-mail: jacques.locat@ggl.ulaval.ca

A.-P. Trottier • P. Lajeunesse
Laboratoire de géosciences marines, Centre d'études nordiques, Université Laval, Québec, QC G1V 0A6, Canada

G. St-Onge
Institut des Sciences de la mer, Université du Québec à Rimouski (ISMER), Rimouski, QC G5L 3A1, Canada

G. Lamarche et al. (eds.), *Submarine Mass Movements and their Consequences*, Advances in Natural and Technological Hazards Research 41,
DOI 10.1007/978-3-319-20979-1_36

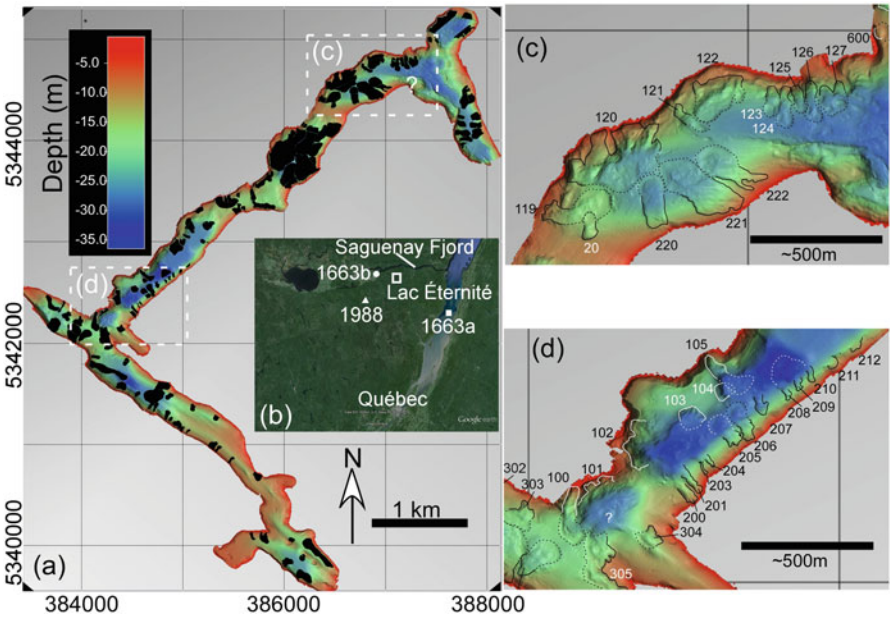

Fig. 36.1 (**a**) Lake Éternité and the landslide coverage in black, note the almost complete disturbance of the lake floor near the central portion of the NE arm; (**b**) Insert showing the location of the Lake Éternité and the position of the reference points referred to in the text (**c**) and (**d**) are examples of basin, located in (**a**), offering accommodation space for landslides. The *dashed line* contours the debris area. *Black* and *white* numbers in '**c**' and '**d**' are slide identification

one of the largest historical earthquake to occur in Eastern Canada with a magnitude Mw of about 7.5, likely the largest for the last 7200 ycal BP (St-Onge et al. 2004), resulting in many aerial and subaqueous landslides (Locat 2011). As part of the review of the 1663 Charlevoix earthquake, there is still some debate about the location of its epicentre (either 1663a or 1663b in Fig. 36.1b) which has significant implications on seismic hazard maps (actual location shown as 1663a in Fig. 36.1b). In his analysis of mass movement signatures in lakes, based on core analysis and shallow seismic survey (no sidescan survey), Doig (1998) suggested that their concentration on SE and SW facing slopes could imply that the epicentre of the earthquake responsible for these mass movements may be located to the NW or NE of the lake.

Therefore, to continue our search for the location of the epicentre of the 1663 earthquake, the work of Doig (1998) will be re-visited in light of more recent research development in this region since 1998, in addition to this 2014 investigation. By doing so, we will also challenge his conclusion that the events noted in Lake Éternité were not related to the 1663 earthquake. At this point, we present our initial analysis of Lake Éternité using two approaches. The first one is based on a morphological analysis of detailed bathymetry map acquired in September 2014 using a GeoSwath interferometric sidescan sonar at a frequency of 250 kHz (1 m resolution) and explored with a 12 kHz shallow seismic echo-sounder. The second approach is a numerical analysis using SPECFEM3D Cartesian software which

uses the continuous Galerkin spectral-element method to simulate elastic wave propagation caused by earthquakes (Komatitsch and Tromp 1999) to look at the effect that source location and topography of the region on the distribution of landslides. It is known that surface topography can significantly affect earthquake ground motion (e.g. Lee et al. 2009a), and SPECFEM3D Cartesian may simulate this effect on a regional scale (e.g. Komatitsch 2004; Lee et al. 2009a, b).

36.2 Geological Setting and Sedimentological Observations

Lake Éternité is located 160 km North of Québec City (Fig. 36.1a). It has a 'T' shape with its longest arm (~5 km) oriented NE-SW. The hills surrounding the lake reach a maximum elevation of 200 m above lake level which is at an altitude of 256 m. The area of the lake covered by the bathymetric survey is 3.8 km^2 (~90 % of the lake total area) with an average width of 0.3 km. The bathymetry is variable with small basins, the deepest one being at a depth of 38 m. The lake geometry is controlled by the underlying bedrock consisting of metamorphic rocks (mostly gneiss) of the Grenville Province that are intensively fractured and faulted. These fractures and faults were later carved by the successive glaciations (Lajeunesse 2014) which are responsible for the 'U' shape valleys in the region, including the Saguenay Fjord. The area was just south of the retreating Wisconsinian ice front about 10,400 years ago (Occhietti et al. 2011).

From the morphology and shallow seismic surveys, the stratigraphic sequence of Quaternary sediments found in lake Éternité consists of till or glacio-fluvial sand and gravel, overlain by glacio-lacustrine sediments which were later covered by a Holocene mud (gyttja). Over the last 2000 years the sedimentation rate in Lake Éternité is about 0.6 mm/year (Doig 1998). The distribution of the glacio-lacustrine sediments may have been controlled by the presence of stagnant ice around which the sediments could accumulate leaving a sort of kettle-like morphology (small basins). So upon the final melting of the stagnant ice, the lake was left with few small basins (e.g. dark blue in Fig. 36.2) often separated by flat lying glacio-lacustrine clays or bedrock sills. In the SE portion of NW-SE arm of the lake, glacio-lacustrine deposition is of less than 1 m and is restricted to shallow basins. As we will see later, most of the small basins provided accommodation space for the accumulation of slide debris resulting from earthquakes.

36.3 Landslide Morphology and Distribution

The distribution of landslides is shown in Fig. 36.1a. A total of 128 landslides have been mapped in the lake. From our knowledge of the region they are believed to have been triggered by earthquakes (Levesque et al. 2006; Dougthy et al. 2014). In most cases, sediments involved consists 2–5 m thick gyttja, seen in seismic profiles

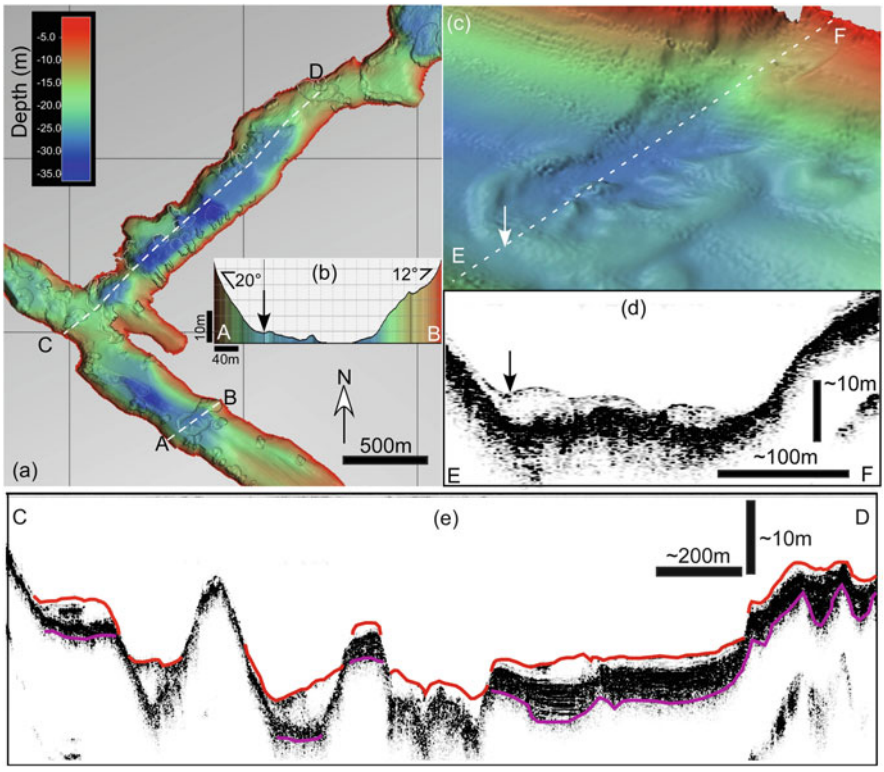

Fig. 36.2 (**a**) A portion of Lake Éternité showing the distribution of the landslides on part of the lake floor; (**b**) A bathymetry profile along *dashed line A–B*; (**c**) 3D view of a landslide with *line E–F* giving the position of the seismic line shown in (**d**), this line is almost at the same position than *line AB* in (**a**); (**d**) a seismic line across the landslide in (**c**); (**d**) An interpreted seismic line along *line C–D* shown in (**a**). The *red line* shows the top of the gyttja transparent layer and the magenta the bottom of the underlying glacio-lacustrine layer. The *arrow* in (**c**) and (**d**) shows the run out distance of the debris of the slide

as a transparent layer draping most of the lake floor (Fig. 36.2e). As shown in Figs. 36.1c, d and 36.2c, almost all slides present a similar morphology: a steep failure surface (10–20°) in the starting zone with an accumulation of mud showing arcuate lobes with a small depression between the back slope and the frontal debris. These debris lobes can be symmetric when they are not in contact with other slides (Fig. 36.2c). For the slide shown in Fig. 36.2b, the head scarp is very close to the shoreline and its height is difficult to define. The rupture surface angle, in the main portion, is about 10° and the run out distance is 290 m. The debris lobe reaches a maximum thickness of about 2.5 m. The estimated volume is 14,000 m^3. In general, scarps are typically less than 2 m high while lateral scarp can reach 3–4 m where the initial morphology had a convex slope near the bottom (as seen in the NW facing slopes along the NE arm). Interestingly, in most basins, gyttja sediments present a

hummocky morphology. To that effect, Shilts and Clague (1992) noted that except for 1 or 2 of the 150 lakes they surveyed in Canada, such a morphology likely resulted from seismic shaking.

Regarding the spatial distribution of landslides, amongst the 128 slides mapped, 71 are on either SE or SW facing slopes while 57 are on NE or NW facing slopes (Fig. 36.1a). The SE facing slopes of the NE arm are more dissected than on the other side of the arm except in a small area where the slopes are flatter or where the underlying bedrock is close to the lake floor.

36.4 Effect of Earthquake Source Location

In order to create a regional Digital Elevation Model, the isohypse (10 m interval) were extrapolated on a 40 m grid, and bathymetric data were added on this map. The mesh used for the numerical simulation, in the preliminary results showed here, have a lower resolution mesh: a grid of 190 m was used. The total simulation area (black square in Fig. 36.3a) consisted in a grid of 216×216 elements, and the domain had a depth of 30 km. As a simplification, velocities for the whole domain were set 4500 and 3500 m/s for primary and secondary wave velocity. The S-wave value is consistent with values determined by Leblanc and Buchbinder (1977).

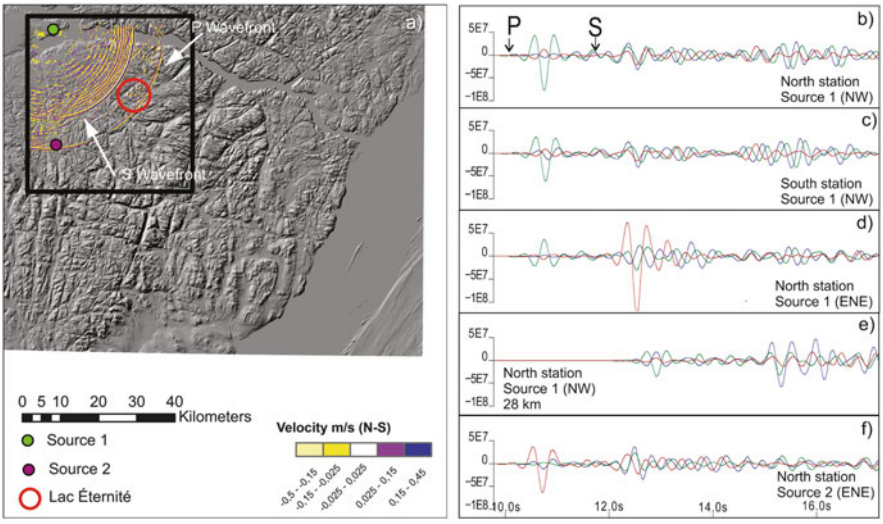

Fig. 36.3 (**a**) Example of seismic wave propagation from source 1; (**b**–**f**) Synthetic seismograms showing the accelerations on the three components (*green* represent the components perpendicular to the shoreline (N315), *red* the component along the shoreline (N45) and *blue* the vertical component) for site located north and south of the main arm of Lake Éternité and for the two sources shown in (**a**). Scale units are not important in this analysis, but all simulations were scaled the same way

However, in order to obtain a more robust model at lower period, the P-wave value was set lower than the standard value that should be around 6000 m/s. Mesh definition in Specfem3D do not allow to model very superficial layers such as the gytjja. Furthermore, since the distance between the source and the receivers is short and authors only want to look at the relative effect of the source location and topography, the rock quality factor was set to 0 (no attenuation), even if the rock is intensely fractured. Two point source areas for the earthquake were simulated (Fig. 36.3a). The first one is located in the Baie des Ha!Ha! (Source 1, Fig. 36.3a), about 25 km NW from the site, the second one is located near the Lake Ha!Ha! (Source 2, Fig. 36.3a), 25 km SW from the site. These two sites were chosen because they are in line with the two main branches of the Lake and because a fault trace visible on aerial photographs that has the same orientation than the presume orientation of the 1988 Chicoutimi earthquake at source 1 was suggested by Locat (2011) to be the fault associated with the 1663 earthquake. Two directions of the source were simulated for source 1: one with the direction of the fault which is approximately to the NW, and another direction consistent with the stress field derived from most focal mechanism of earthquakes elsewhere in eastern Canada, i.e. N60E (Adams and Basham 1989). For source 2, the direction of the source was set to be N60E. The point source simulated has a force of 1×10^{21} N and the hypocenter was at a depth of 12 km. This depth was chosen as most earthquakes in this area (more specifically in the Charlevoix-Kamouraska zone) have their hypocenter at a depth between 5 and 15 km (Boore and Atkinson 1992) with a median depth of 12 km (Lamontagne 1999). One simulation was also made with a depth of 28 km, which was the depth of the 1988 earthquake, the biggest earthquake that was recorded in this area. Figure 36.3a shows an example of the propagation of the wave for a simulation made with the epicenter at the Baie des Ha!Ha!. This figure shows the N-S speed component at the surface in m/s.

Results from five different simulations will be presented. The first three simulations have their source in the Baie des Ha!Ha!, but for simulation (1), the direction of the source is set to be the direction of the fault, simulation (2) uses the N60E source direction, and simulation (3) uses the same setting as (1) but with a depth of 28 km. The fourth simulation used the same setting as simulation (2), but the source was moved to the Lake des Ha!Ha!.

Synthetic seismograms were calculated in the model on both sides of the Northern arm of Lake Éternité (Fig. 36.2a). The seismograms were filtered with a Butterworth filter, where the period between 0.35 and 10 s was kept. The smaller period correspond to the shortest period where the model was found stable. Figure 36.3 shows the results of four different simulations. In (b) and (c) are shown the results for the first simulation from the north side and the south side of the northern branch. Figure 36.3d shows the results for the north side of the lake, but for the second simulation. Figure 36.3e shows the results for the north side for the third simulation, and Fig. 36.3f shows the results, again for the north side, but when the source is moved to the Lake des Ha!Ha!.

36.5 Discussion

The distribution of landslides around the lake could support the effect of the orientation of the lake relative to the seismic source at the origin of these slides. We could make the hypothesis that they were triggered by the largest events since 7200 ycal BP, i.e. the 1663 Charlevoix earthquake. Doig (1998), using short sediment cores conclude that he could see re-suspended sediments form the 1988 Saguenay earthquake but not for the 1663 one, although he could see the record of an older one, about 1200 years ago. Doig (1998) paper could not take into account the many studies carried out since that time which showed that there are many very large landslides events, related to the 1663 earthquake, in the Upper Saguenay Fjord area (Locat 2011). In addition, the position of the cores used by Doig (1998) is not known and considering the very disturbed nature of the lake floor this is very important to know. In his 1990 and 1998 papers, Doig indicate that his method would better in lakes were there are no landslides, which is not the case. With our current detailed bathymetry, it would now be much easier to select a site with minimum interference with nearby slope movements. We should also keep in mind the results of the work of Levesque et al. (2006) who showed that for the Saguenay Fjord the initial hypothesis that all slide scars were caused by the 1663 earthquake was only valid for 6 of 17 sites investigated. As it was done by Levesque et al. (2006) future work on Lake Éternité will focus on coring at various landslides sites (on the rupture surface and in undisturbed areas) to establish a reliable chronology considering that major earthquakes occurred also in 1791 ($M6$), 1860 ($M6$), 1871 ($M6.5$), 1925 ($M6.2$) and 1988 ($M5.9$) (Levesque et al. 2006).

The effects of the topography on site response were observed at various locations, such as in California (Spudich et al. 1996), where a site, 15 m high, 500 m long and 130 m wide, instrumented with multiple geophones, was subjected to an earthquake. They showed that at the top of the hill amplifications were more than three to four times higher than at the base of the hill. In the simulations presented here, there was no noticeable difference between the seismograms presented with or without topography, as well as between seismograms on the two sides of the Lake, at the same elevation.

Based on Fig. 36.3b, c, showing the difference between the acceleration on the northern side and the southern side of the lake, we can conclude that, at least with the resolution of the mesh that was used here, the effect of topography between the north and south shores, is present but negligible. Furthermore, the acceleration along the coastline direction (red) is approximately the same as the acceleration perpendicular to the coastline direction (green), except for the P waves, where the acceleration perpendicular to the coastline is much higher than along the coastline. For both seismograms, the highest acceleration is caused by the arrival of P waves, and the acceleration on the north station is slightly higher than at the south station. The main reason that may explain this small difference, may be the resolution of the mesh used in the simulation that is too coarse to capture greater amplification. With a minimum period resolved of 0.35 s and a S-wave speed of 3500 m/s, minimum

wavelength resolved of the S-wave will be of 1225 m. Topographic effects would probably not be resolved for height difference of less than a quarter of this wavelength.

Three other factors must be taken into account: the source location, its depth and the direction of the source. As for the source directivity, Raghukanth et al. (2012), in their regional study of landslides associated with the 2011 Sikkim Earthquake near the border of Nepal and the Indian state of Sikkim, found correlations between the simulated ground motion obtained with simulations made with SPECFEM3D and landslide locations. Furthermore, they showed a correlation between the displacement and the directivity effect due to the fault orientation and rupture direction at specific sites.

The direction of the source was taken into account by simulations 1 and 2 where the source was kept constant, but the direction of the source was moved from the NW to the ENE (Fig. 36.3b, d). Major differences may be seen for both the P wave and the S wave. For the P wave, the acceleration, when the source is in the ENE direction, is about half the acceleration of the simulation 1. However, when the source is in the ENE direction (Fig. 36.3d), the amplitude of the acceleration in the direction perpendicular to the shoreline as well as in the vertical direction, for the P waves will be slightly higher than when the source is in the NW direction. The alongshore component will be three to four times higher when the source is to the ENE.

Scenarios 1 and 3, i.e. Fig. 36.3b, e, show the influence of the depth of the source. When the source is deeper, the horizontal components will be slightly lower; however, the vertical component will be higher.

The effect of source location is well seen in the simulations. Comparison of Fig. 36.3d, f, i.e. seismograms for the same station location but with a different source, shows that the signal is also dependant on the source location. On Fig. 36.3f, for the P wave, the component along the coastline is the major component, which is the opposite of what is seen in Fig. 36.3e. For the P waves, for source 2, the amplitudes in all three directions are about the same, which is very different than at source 1 where the component along the coastline direction is way higher. In all cases, the maximum acceleration amplitudes seen are lower when the source is near the Lake des Ha!Ha!.

36.6 Concluding Remarks

The following remarks can be made from our initial analysis of geomorphological and geophysical data at Lake Éternité and a regional wave propagation numerical modeling:

1. The great disturbance of the gytjja by the earthquakes(s) resulted in more than 128 landslide scars with volume from 3000 to 15,000 m^3.

2. There are more slide scars on the SE and NW facing slopes. Dating these slides and their associated earthquakes could be used to map their relative spatial occurrence and validate or not the hypothesis that the epicentre of the 1663 earthquake could be located to the NW or NE of the lake, i.e. towards the Saguenay Graben.
3. Preliminary numerical simulations suggest that, at least at the resolution of the model, the topography does not appears to play a significant role as a seismic amplification factor. However, only regional simulations were run and the resolution of the model had to be kept coarse. Simulations with a smaller domain but with a higher resolution will need to be run. On the other hand, the numerical simulations clearly illustrate the effect of the directivity of the source and of its position. For a position of the source based on Locat (2011), for both direction of the source, the acceleration for all components are higher than when the source is near the Lake des Ha!Ha!. More numerical analysis along these lines will be carried in a near future. Modification of the source position to be at the position of the 1988 earthquake, 50 km from the Lake des Ha!Ha!, as well as more local simulations, will need to be done.

Acknowledgments The authors would like to thank the Association of Lac Éternité for providing access to the lake and to NSERC for their funding support. We also thank Nabil Sultan and Didier Perret for their constructive review of the manuscript.

References

Adams J, Basham P (1989) The seismicity and seismotectonics of Canada east of the Cordillera. J Geol Assoc Can 16(1):3–16

Boore DM, Atkinson GM (1992) Source spectra for the 1988 Saguenay, Quebec, earthquakes. Bull Seismol Soc Am 82(2):683–719

Doig R (1990) 2300 yr history of seismicity from silting events in Lake Tadoussac, Charlevoix, Quebec. Geology 18:820–823

Doig R (1998) 3000-year paleoseismological recods from the region of the 1988 Saguenay, Québec, earthquake. Bull Seismol Soc Am 88(5):1198–1203

Dougthy M, Eyles N, Eyles CH, Wallace K, Boyce JI (2014) Lake sediments as natural seismographs: earthquake-related deformation (seismites) in Canadian lakes. Sediment Geol 313:45–67

Komatitsch D (2004) Simulations of ground motion in the Los Angeles Basin based upon the spectral-element method. Bull Seismol Soc Am 94(1):187–206

Komatitsch D, Tromp J (1999) Introduction to the spectral element method for three-dimensional seismic wave propagation. Geophys J Int 139(3):806–822

Lajeunesse P (2014) Buried preglacial fluvial gorges and valleys preserved through Quaternary glaciations beneath the eastern Laurentide Ice Sheet. Geol Soc Am Bull 126:447–458

Lajeunesse P, St-Onge G, Randall K, Moreau-Labrecque A (2008) Mouvements de masse subaquatiques postglaciaires au lac Jacques-Cartier, Réserve faunique des Laurentides (Québec): résultats préliminaires. Comptes rendus de la 4e Conférence canadienne sur les géorisques: des causes à la gestion. Presse de l'Université Laval, Québec 313–321

Lamontagne M (1987) Seismic activity and structural features in the Charlevoix region, Quebec. Can J Earth Sci 24:2118–2129

Lamontagne M (1999) Rheological and geological constraints on the earthquake distribution in the Charlevoix Seismic Zone, PhD. thesis, Carleton University, Ottawa, 353 pp
Leblanc G, Buchbinder GGR (1977) Second micro-earthquake survey of the St. Lawrence Valley near La Malbaie, Quebec, Canada. Can J Earth Sci 14:2778–2789
Lee SJ, Chan YC, Komatitsch D, Huang BS, Tromp J (2009a) Effects of realistic surface topography on seismic ground motion in the Yangminshan Region of Taiwan based upon the spectral-element method and LiDAR DTM. Bull Seismol Soc Am 99(2A):681–693
Lee SJ, Komatitsch D, Huang BS, Tromp J (2009b) Effects of topography on seismic-wave propagation: an example from Northern Taiwan. Bull Seismol Soc Am 99(1):314–325
Levesque CL, Locat J, Leroueil S (2006) Dating submarine mass movements triggered by earthquakes in the upper Saguenay Fjord, Quebec, Canada. Nor J Geol 86:231–242
Locat J (2011) La localisation et la magnitude du séisme du 5 février 1663 (Charlevoix) revues à l'aide des mouvements de terrain. Rev Can Géotech 48:1266–1286
Normandeau A, Lajeunesse P, Philibert G (2013) Late-Quaternary morphostratigraphy of Lake St-Joseph (southeastern Canadian shield): evolution from semi-enclosed glacimarine basin to a postglacial lake. Sediment Geol 295:38–52
Occhietti S, Parent M, Lajeunesse P, Robert F, Govare E (2011) Late Pleistocene-early Holocene decay of the Laurentide ice sheet in Québec-Labrador. In: Ehlers J, Gibbard PL, Hughes PD (eds). Elsevier, Netherlands, Developments in Quaternary science, vol 15. pp 601–630
Raghukanth STG, Lakshmi K, Kavitha B (2012) Estimation of ground motion during the 18th September 2011 Sikkim Earthquake, earthquake. Geomatics Risk 3(1):9–34
Shilts WW (1984) Sonar evidence for postglacial tectonic instability of the Canadian Shield and Appalachians. Curr Res Pt A Geol Surv Can Pap 84-1A:567–579
Shilts WW, Clague JJ (1992) Documentation of earthquake induced disturbance of lake sediments using sub-bottom acoustic profiling. Can J Earth Sci 29:1018–1042
Spudich P, Hellweg M, Lee WHK (1996) Directional topographic site response at Tarzana observed in aftershocks of the 1994 Northridge, California, Earthquake: implications for mainshock motions. Bull Seismol Soc Am 86(1b):S193–S208
St-Onge G, Mulder T, Piper DJW, Hillaire-Marcel C, Stoner S (2004) Earthquake and flood-induced turbidites in the Saguenay Fjord (Québec): a Holocene paleoseismicity record. Quat Sci Rev 23(3–4):283–294. doi:10.1016/j.quascirev.2003.03.001